Micro-slip field at a rough contact driven towards macroscopic sliding

Julien Scheibert, Georges Debregeas, Alexis Prevost

Micro-slip field at a rough contact driven towards macroscopic sliding

J. Scheibert, G. Debrégeas, A. Prevost*
Laboratoire de Physique Statistique de l'ENS, UMR 8550,
CNRS-ENS-Universités Paris 6 and 7, 24 rue Lhomond F-75231 Paris, France
(Dated: September 18, 2008)

The incipient sliding of a multicontact interface between a smooth glass sphere and a rough elastomer block is studied using an image correlation velocimetry technique. The displacement field of the elastomer's surface is measured both inside and outside the apparent contact region with a submicrometer displacement resolution. For a given shear load, a coexistence between an inner stick region surrounded by an outer slip annulus is observed. The stick region extension decreases with increasing load and eventually vanishes at the sliding threshold. These measurements allow for the first quantitative test of Cattaneo and Mindlin (CM) classical model of the incipient sliding of a smooth interface. Small deviations are observed and interpreted as a result of the finite compliance of the rough interface, a behavior which contrasts with Amontons' law of friction assumed to be valid locally in CM's model. We illustrate how these measurements actually provide a method for probing the rheology of the rough interface, which we find to be of the elasto-plastic type.

PACS numbers: 46.55.+d, 61.41.+e, 62.20.Qp, 68.35.Ct
Keywords: Contact mechanics, friction law, incipient sliding, micro-slip, image correlation velocimetry technique, multicontact, interfacial rheology

Amontons' law of friction states that the shear force required to trigger relative sliding between two solids in contact is proportional to the applied load normal to the interface. However, it is known that even for minute shear forces, well before macroscopic sliding settles in, micro-slip occurs within the contact. Slip bearing regions are thus expected to coexist with adhesive ones and to progressively invade the contact as the shear force approaches the sliding threshold. Providing a proper local description of this incipient sliding regime remains challenging despite its importance to the fields of tribology [1], earthquakes nucleation [2] or mechanical engineering [3, 4]. In the case of spherical contacts between elastic bodies (Hertz contact), an analytical solution to this problem is given by Cattaneo and Mindlin's (CM) procedure which has now become a classical model for shear loaded frictional contacts below the sliding threshold. It predicts that the stick region is a central disk whose radius continuously decreases from the apparent contact zone radius down to zero upon increasing shear loading [5, 6]. Experimental confirmation of CM's predictions has been obtained only indirectly by measuring macroscopic force-displacement curves or by observing the fretting zone resulting from the interfacial micro-slip [7].

In CM's approach, the interface is assumed to be smooth, incompressible and to obey locally Amontons' rigid-plastic like friction law. This is at odds with most realistic situations where surfaces are rough down to the micrometer scale, resulting in a multicontact interface with a much richer mechanical response [8, 9, 10, 11, 12]. One may wonder how these characteristics modify CM's predictions. In this Letter, we address this question by probing the local displacement field at a contact between a rigid sphere and a rough elastomer block for which displacements can be measured with a submicrometer resolution using an image correlation velocimetry technique. This method directly makes use of the micro-junctions and micro-asperities present at the interface as markers.

The sphere is an optically smooth glass lens (radius of curvature $R = 128.8$ mm) and the elastomer block (50×50 mm, thickness $h = 15$ mm) is made of a crosslinked PolyDimethylSiloxane (PDMS Sylgard 184, Dow Corning, Young's modulus $E = 2.2 \pm 0.1$ MPa, Poisson ratio ν=0.5). Its surface has been rendered rough by moulding the cross-linker/PDMS melt against a Plexiglas surface mechanically abraded with an aqueous solution of SiC powder. Its topography was characterized with optical profilometry (M3D, Fogale Nanotech). Its power spectral density is a power law down to the micrometer scale and up to about 40 μm. Its characteristic thickness σ, taken as the standard deviation of the height distribution, was found to be $1.28 \pm 0.05\,\mu$m. Both glass and PDMS surfaces were cleaned with ethanol and dried with filtered air prior to any experiment.

A typical experiment consists in pulling the elastomer block in contact with the sphere under a prescribed normal load P at constant velocity V with a precision motorized actuator (LTA-HL, Newport), while recording simultaneously P, the shear load Q and images of the interface (Fig. 1). In all experiments, $V = 4\,\mu$m/s, a velocity small enough for visco-elastic interfacial dissipation to be negligible [13]. Both P and Q are measured at a sampling rate of 1 kHz by probing with position sensors the deflections of two cantilevers (Fig. 1, lower inset). The normal loading of the contact produces a significant shear force due to the coupling between normal and lateral motion of each cantilever. To circumvent this problem the contact is manually renewed until Q is less than 1% of P. During this separation procedure, no measurable pull-off force is observed, indicating that adhesion forces are neg-

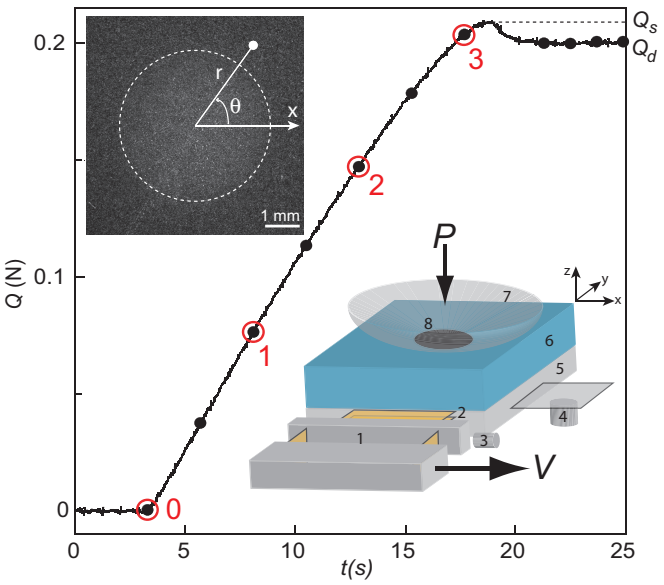

FIG. 1: (Color online) Sketch of the experimental setup (lower inset), time evolution of the shear force Q during the loading experiment with $P = 0.33$ N and $V = 4\,\mu$m/s, and image of the contact (upper inset) with its apparent contact border (white dashed line) and coordinates system. On the sketch, (1) is the shear cantilever (stiffness 9579 ± 25 N.m^{-1}) and (2) the normal one (stiffness 689 ± 5 N.m^{-1}), (3) and (4) are two capacitive position sensors (MCC10 and MCC20, Fogale Nanotech), (5) is a glass plate to which the PDMS block (6) is attached, (7) is the glass lens and (8) the resulting circular contact. On the Q curve, circled points and black disks indicate Q values at which the displacements are displayed in the next figures.

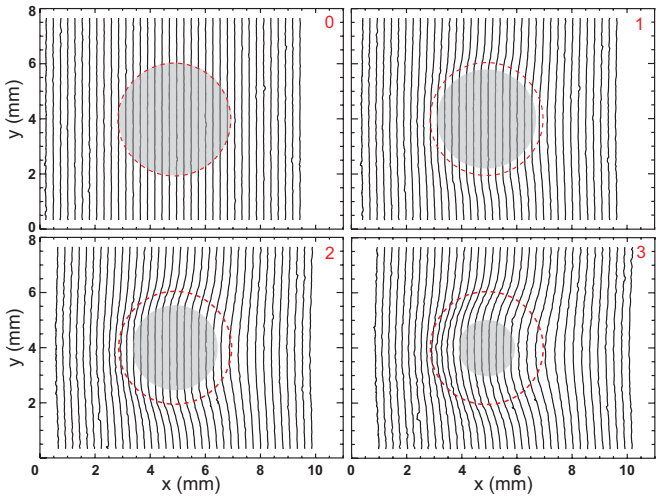

FIG. 2: (Color online) Snapshots of the displacement field $u_x(x, y)$ at the positions labeled 0, 1, 2 and 3 on the curve of Fig. 1. The reference, undeformed image is taken at position 0. $u(x, y)$ is represented by joining together with a solid line the extremities of the displacement vectors $\vec{u_x}$ of equal abscissa grid points. Since u_x lies in the range [0, 100 μm] an amplification factor of 30 has been used to ease vizualisation. The dashed circle is the border of the apparent contact region whose area is unaffected by the loading. The grey circular disk is a region of null displacement within the contact.

ligible [14, 15]. Q versus time curves, like the one shown in Fig. 1 for $P = 0.33$ N are reproducible for any P in the experimentally accessible range [0, 1 N], with the following typical behavior. While P varies by less than 1%, Q increases until it reaches a maximum value Q_s beyond which it slightly decreases before flattening at a constant value $Q_d = 0.96\,Q_s$ signaling a steady sliding regime with a dynamical coefficient of friction of about 0.6.

Imaging of the contact is done by illuminating the optically transparent PDMS block from below with a white LED and a ground glass diffuser, and using a stereomicroscope (Olympus SZ11). Images (Fig. 1, upper inset) are recorded by a CCD camera (Hamamatsu C8484-05G, 12 bits), whose 1344×1024 pixels sensor provides at the chosen magnification a field of view of 9.8×7.5 mm. Images' contrast results from the diffusive nature of the rough interface. In the contact region, additional bright spots correspond to the micro-junctions which favorably transmit light. Interfacial displacement fields are extracted from snapshots acquired at a 4 Hz frame rate using an image correlation velocimetry technique [16, 17].

It consists in finding, for a given subimage at position (x, y) in a reference image the displacement (u_x, u_y) which provides the maximum correlation with a subsequent deformed image. Since u_x is at least an order of magnitude larger than u_y, the correlation function is calculated by translating a square window of side length λ along the shear direction x only. With $\lambda = 20$ pixels, the u_x field is obtained with a spatial resolution of about 150 μm. The resolution on the displacements, found by correlating two different images of the interface prior to contact, and taken as the standard deviation of the displacements distribution, is about 275 nm, i.e. $1/30^{th}$ pixel. All displacements are defined respective to an image taken at $Q = 0$ N.

The displacement field at various applied forces along the loading curve of Fig. 1 was determined by correlating successive images with the $Q = 0$ reference image and is shown in Fig. 2 at four instants. For a given Q a central circular stick region coexists with a surrounding annulus in which slip has already occured. Its diameter decreases with Q and vanishes at Q_s. When $Q = Q_d$, u_x is the sum of two terms. The first one corresponds to the driving motion and is a uniform displacement of amplitude Vt. The second one is a residual displacement corresponding to the deformation of the elastomer block (Fig. 3, insets).

Such a scenario has been theoretically predicted by Cattaneo and Mindlin (CM) [5, 6] who have considered the combined normal and shear loading of a contact between spherical elastic bodies. Their calculations assume that (1) both surfaces are *smooth*, (2) the pressure distribution p within the contact is unchanged upon shearing

and given by Hertz contact theory, and (3) Amontons' law of friction is valid locally at any (r, θ) position (Fig. 1, upper inset), i.e. slip occurs wherever the shear stress q reaches μp, μ being the friction coefficient. For a contact of radius a between a rigid sphere of radius R and an elastic plane of reduced modulus $E^* = \frac{E}{1-\nu^2}$ under normal load P, $p(r, \theta)$ is given by $p(r) = p_0\sqrt{1 - r^2/a^2}$ with $p_0^3 = \frac{6PE^{*2}}{\pi^3 R^2}$. CM predicts the coexistence of an inner adhesive circular region of radius $c = a\left(1 - Q/(\mu P)\right)^{1/3}$ surrounded by an outer slip annulus. Using a superposition principle, CM's calculations provide complete analytic expressions for u_x within the contact, in both the stick and slip regions [3, 4]. Further derivations by Johnson [3] also give u_x outside the contact, thus providing the entire field at the interface. Comparison between CM's and measured u_x were done in two ways, by averaging $u_x(r, \theta)$ over θ (Fig. 3(a)), and by evaluating $u_x(a, \theta)$ with θ running from 0 to 2π (Fig. 3(b)).

In Fig. 3(a), displacement curves are shown for all values of Q corresponding to the dotted positions along the Q curve in Fig. 1. The inset shows $u_x(r) - u_x(0)$ in the steady sliding regime at the last four dotted points. Evaluation of $u_x(a, \theta)$ (Fig. 3(b)) is done similarly at the same dotted points in the transient loading regime and in steady sliding (inset). As shown, a good overall agreement between CM's predictions (red solid lines) and the measured u_x is found. Close look at their radial dependence even shows that the radius of the stick region is very close to CM's prediction for c. In addition, CM's expressions for $u_x(a, \theta)$ predict a $cos(2\theta)$ dependence, which is well reproduced over the whole θ range and for all Q.

Systematic deviations to CM's predictions are however clearly seen on the radial profiles displayed in Fig. 3(a). Outside the stick region ($r > c$), the experimental data points systematically lay below the predicted profiles. Furthermore, while CM's model predicts a kink in the radial displacement profiles at $r = a$, the measured curves remain smoother. This may be attributed to deviations to Hertz's pressure field around $r = a$, induced by the non-linear normal compressibility of the rough layer [9]. More surprisingly, in the stick region ($r < c$) a non-zero displacement in the submicrometric range is measured whose value increases with Q. This effect can be best caught by evaluating $u_x(r = 0)$ averaged over a disk of radius λ centered on the contact as a function of time. Results plotted in Fig. 4(a) and magnified on Fig. 4(b) show that in the loading phase $u_x(r = 0)$ increases continuously from 0 to about 1 μm.

This can be understood when considering that the image correlation velocimetry technique actually probes the mean displacement over the mean thickness σ of the rough layer. It indeed averages out intensity fluctuations due to both the micro-contacts and the non-contacting micro-asperities between micro-contacts. We can then

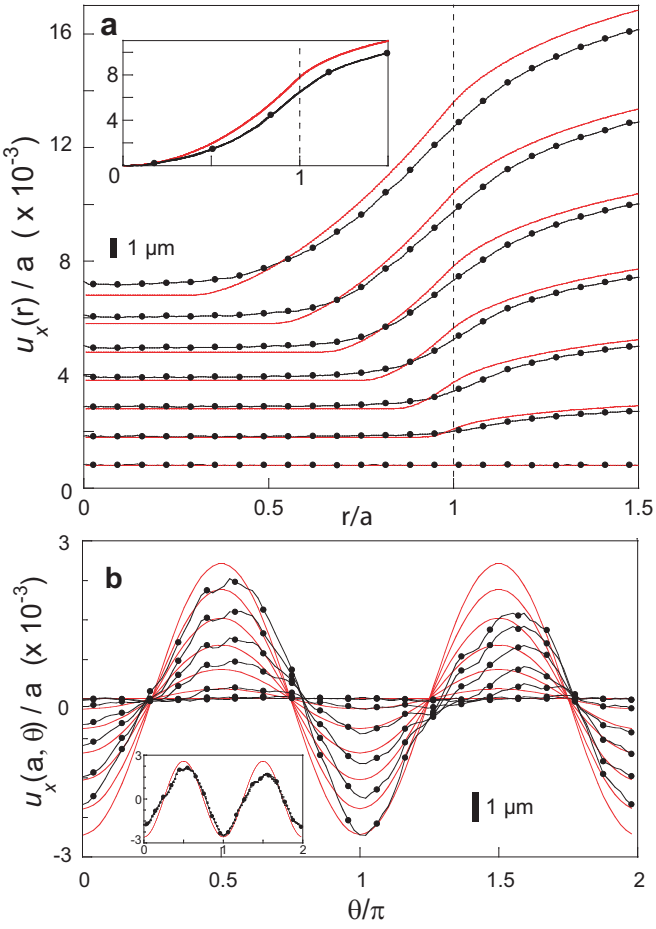

FIG. 3: (Color online) Comparison between the measured displacements (solid lines with filled disks) and CM's predictions (red solid lines). (a) $u_x(r)/a$ versus r/a. All curves are shifted arbitrarily along the y axis for vizualization and CM's curves have been smoothed out with a running window of size λ. From bottom to top, each set of curves corresponds to an increasing Q in the loading phase (black dots in Fig. 1). Inset shows 4 almost fully overlapped $u_x(r)/a$ curves in steady sliding measured at the last 4 dotted positions in Fig. 1. (b) $u_x(a, \theta)/a$ versus θ evaluated at the same Q in the transient regime, and in steady sliding (inset).

propose the following scenario. As long as $Q < Q_s$, summits of the asperities in contact remain stuck [22] while their underlying bulk base is displaced due to the applied shear. The rough layer is therefore deformed with a mean strain which can be estimated, at the center of the contact, as $\epsilon_0 = u_x(r = 0)/\sigma$ (Fig. 4(c)). The image correlation velocimetry technique developped here thus appears as a tool to probe locally the rheology of the rough layer, provided that the corresponding shear stress q_0 is known. Since our experiment does not allow any direct shear stress measurement, we have used CM's prediction for $q_0 = q(r = 0) = \mu p_0(1 - c/a)$ to obtain q_0 versus ϵ_0 (Fig. 4(d)). Clearly, the rough layer mechanical response deviates significantly from the Amontons'

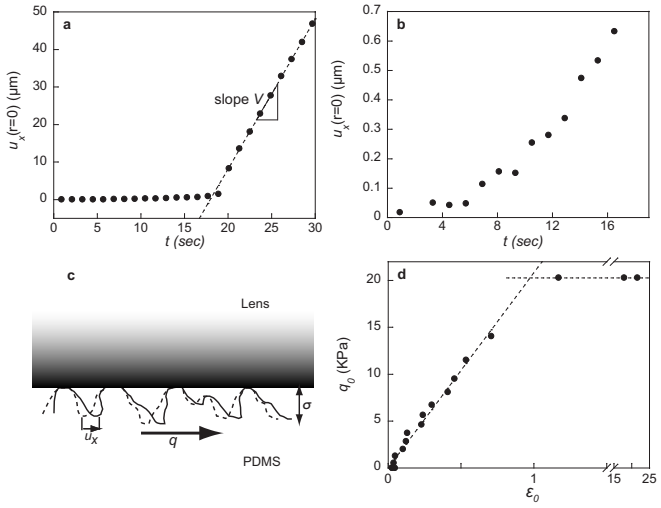

FIG. 4: (a) $u_x(r = 0)$ versus time. The dashed line is a linear fit, characterizing steady sliding at $V = 4\,\mu$m/s. (b) Magnified centered region of the previous plot. (c) Sketch detailling the mechanism resulting in a non-zero measured displacement in the stick region. (d) Calculated shear stress q_0 at $r = 0$ using CM's model versus the strain ϵ_0 defined as $u_x(r = 0)/\sigma$. Shown in dashed lines are the $q_0 = 20$ kPa horizontal line and a linear fit of the data points for $\epsilon_0 < 1$.

rigid-plastic like behavior assumed by CM. The friction law is rather elasto-plastic like with an effective shear modulus G_l given by $G_l = \partial q_0/2\partial\epsilon_0$ of about 10 kPa. This value is two orders of magnitude smaller than the bulk shear modulus $G = \frac{E}{2(1+\nu)} \approx 0.73$ MPa. It is fully consistent with previous measurements on multicontacts averaged over the whole apparent contact area [10]. It is expected to depend on the local pressure so that systematic measurements at successive different loads would be required to determine the complete mechanical response of the rough layer.

In this Letter we have implemented an image correlation velocimetry technique to measure with a submicrometer resolution the displacement field at a multicontact interface between a soft elastomer and a rigid body. This technique provides the first direct and non-invasive measurements of the interfacial slip field in both incipient sliding and steady sliding regimes at a sphere-on-plane contact. It can be directly applied to dynamical regimes, therefore complementing real contact area measurements on rough contacts such as those recently implemented in Plexiglas to investigate the interfacial dynamics of a multicontact interface at the onset of sliding [18, 19]. In principle, it could also be extended to smooth contacts by patterning the elastomer with markers located below its surface [20]

The measured displacement fields are well captured by the classical model of Cattaneo and Mindlin thus providing its first direct experimental test. Significant deviations are however observed and shown to result from the too stringeant smoothness assumption, which is often made in continuum mechanics calculations. The interfacial rough layer indeed exhibits a finite shear compliance. The latter was directly probed, allowing to evidence an elasto-plastic like friction law different from Amontons' law which is commonly believed to apply for multicontacts. These results provide direct experimental support to the interpretation of a recently observed non-Amontons behavior in a similar setup [21].

The auhors wish to thank Antoine Chateauminois and Christian Frétigny for fruitfull discussions.

* alexis.prevost@lps.ens.fr

[1] T. Baumberger and C. Caroli, Adv. Phys. **55**, 279 (2006).
[2] Y. Ben-Zion, J. Mech. Phys. Solids **49**, 2209 (2001).
[3] K. L. Johnson, *Contact Mechanics* (C. U. P., 1985).
[4] D. Hills and D. Nowell, *Mechanics of Fretting Fatigue* (Kluwer Academic Publishers, 1994).
[5] C. Cattaneo, Rendiconti dell'Accademia nazionale dei Lincei **27**, 214 (1938).
[6] R. D. Mindlin, Trans. ASME, Series E, J. Appl. Mech. **16**, 259 (1949).
[7] K. L. Johnson, Proc. R. Soc. London, Ser. A **230**, 531 (1955).
[8] J. A. Greenwood and J. B. P. Williamson, Proc. R. Soc. London, Ser. A **295**, 300 (1966).
[9] J. A. Greenwood and J. H. Tripp, Trans. ASME, Series E, J. Appl. Mech. **34**, 153 (1967).
[10] P. Berthoud and T. Baumberger, Proc. R. Soc. London, Ser. A **454**, 1615 (1998).
[11] B. Persson, Phys. Rev. Lett. **99**, 125502 (2007).
[12] M. Müser, Phys. Rev. Lett. **100**, 055504 (2008).
[13] O. Ronsin and K. L. Coeyrehourcq, Proc. R. Soc. London, Ser. A **457**, 1277 (2001).
[14] K. R. Shull, Mat. Sci. Eng. R. **36**, 1 (2002).
[15] K. N. G. Fuller and D. Tabor, Proc. R. Soc. London, Ser. A **345**, 327 (1975).
[16] F. Hild and S. Roux, Strain **42**, 69 (2006).
[17] J. Scheibert, *Mécanique du contact aux échelles mésoscopiques* (Edilivre, Collection Universitaire, 2008).
[18] S. M. Rubinstein, G. Cohen, and J. Fineberg, Nature **430**, 1005 (2004).
[19] S. Rubinstein, G. Cohen, and J. Fineberg, Phys. Rev. Lett. **96**, 256103 (2006).
[20] A. Chateauminois and C. Frétigny, Private communication (2008).
[21] J. Scheibert, A. Prevost, J. Frelat, P. Rey, and G. Debrégeas, Europhys. Lett. **83**, 34003 (2008).
[22] Direct confirmation that the micro-contacts remain stuck was obtained by zooming on individual asperities.